Growth of Transparent and Conductive Polycrystalline (0001)-ZnO Films on Glass Substrates Under Low-Temperature Hydrothermal Conditions

*Matejka Podlogar, Jacob J. Richardson, Damjan Vengust, Nina Daneu, Zoran Samardžija, Slavko Bernik, and Aleksander Rečnik**

Flat panel display technology seems to be an ever-expanding field developing into a multibillion dollar market. A set of technical solutions involve a transparent conducting film (TCF) that is today still dominated by indium-tin-oxide (ITO). In a race to find alternatives that would avoid the indium pitfalls, mainly due to its increasing price and limited natural availablity, replacement materials have been extensively investigated. This work demonstrates that by exploiting basic principles of crystal growth in geometrically constrained conditions, zinc oxide (ZnO) could easily be utilized for this purpose. ZnO layers were grown on inexpensive glass substrates via low-temperature citrate-assisted hydrothermal (HT) method. It was shown that in the nucleation stage the crystal growth can be efficiently controlled by spatially confined oriented growth (SCOG) mechanism to produce smooth and dense (0001) oriented polycrystalline ZnO films with superb optical properties. Our products show optical transparency of 82% and surprisingly low sheet resistance for undoped ZnO, only in the order of few 100 Ω sq^{-1}. We believe that a very high degree of self-organization between the ZnO crystals in our polycrystalline films grown under controlled SCOG conditions is main reason for the highest so far reported transparency to conductivity ratio for undoped ZnO thin film ceramics.

1. Introduction

Zinc oxide (ZnO) has generated a lot of interest in materials science due to its attractive physical properties and diverse technological applications.[1] Properties of polycrystalline ZnO depend on its microstructure, including grain size, crystal morphology, orientation and crystal aspect ratio, total surface area, pore distribution and the nature of the interfaces. Due to a wide direct band gap of 3.3 eV at room temperature and a large exciton binding energy of 60 meV ZnO is a promising material for photonic and electronic applications. Potential applications for ZnO have been demonstrated in light emitting diodes,[2] transparent conductive electrodes,[3] gas sensors,[4] piezoelectric nanogenerators,[5,6] etc. Optically transparent and electrically conductive ZnO films are good candidates to replace ITO (indium-tin-oxide) films, which are used for liquid crystal and plasma displays, touch panels, organic light-emitting diodes, gas sensors, anti-static and anti-reflection coatings, solar cells, *etc.*

ZnO films can be deposited onto substrates by a variety of methods. Deposition is typically performed by vapor-based techniques including carbothermal evaporation,[7] sputtering,[8] pulsed laser deposition (PLD),[9] molecular beam epitaxy (MBE),[10] atomic layer deposition (ALD),[11] and chemical vapor deposition (CVD).[12–14] However, most of these techniques have serious drawbacks, such as complicated processing that generally involves a high cost equipment, expensive single crystal substrates, the need of high temperatures and high vacuum conditions for a relatively low yield, which limit their wide technological application. The increasing demand of the market towards the use of temperature sensitive substrates, such as glass and polymers, required film deposition at lower temperatures. To address the drawbacks of vapor deposition methods solution-based methods of film deposition such as electrochemical deposition and precursor based solution deposition techniques, like sol-gel or chemical solution deposition (CSD), have been studied extensively. These approaches, however, have some issues: electrochemical deposition requires a conductive substrate like metal,[15] ITO,[16] or graphite,[17] whereas sol-gel and CSD require annealing to obtain high quality films.[18,19]

Recently it was demonstrated that layers of ZnO crystals can be grown on different substrates directly from low-temperature aqueous solutions.[20] Solvothermal methods,

M. Podlogar, Prof. N. Daneu, Dr. Z. Samardžija, Prof. S. Bernik, Prof. A. Rečnik
Department for Nanostructured Materials and Centre of Excellence NAMASTE
Jožef Stefan Institute
Jamova cesta 39
Ljubljana, 1000, Slovenia
E-mail: aleksander.recnik@ijs.si
Dr. J. J. Richardson
Materials Department
University of California at Santa Barbara
Santa Barbara, CA 93106, USA
D. Vengust
Department for Complex Matter
Jožef Stefan Institute
Jamova cesta 39, Ljubljana, 1000, Slovenia

DOI: 10.1002/adfm.201200214

known as hydrothermal (HT),[21] or chemical-bath deposition (CBD),[22] have many advantages over the vapor- and other solution-based deposition techniques, such as easy implementation on the industrial scale, near atmospheric-pressure and low-temperature processing, lower cost of equipment, possibility to use a wide range of substrates and it is also environmentally benign. Initially, the research was focused on the growth of various ZnO nanostructures rather than continuous ZnO films. When ZnO is nucleated and grown from an aqueous solution in a single step, the result is a relatively low density of more or less randomly oriented acicular ZnO crystals.[20] This is a consequence of ZnO's natural tendency to grow much faster in the [0001] direction than in the perpendicular directions, resulting in needle- or wire-like morphology of ZnO crystals. However, if a ZnO seed layer is deposited on the substrate prior to the HT step, the quality of ZnO films can be drastically improved. Seed layers can be prepared in several ways, including dehydration of Zn-O precursors,[20,23–27] ALD,[28] radiofrequency (RF) magnetron sputtering method,[29] among others. Greene *et al.*[23] demonstrated a simple method to prepare seed layer using a Zn-acetate precursor film. The density and the size of ZnO nuclei is important to control the crystal growth under HT conditions. High density of nuclei leads to the formation of continuous ZnO films consisting of densely packed hexagonal ZnO rods, however if the density is low, spatially separated and tilted ZnO rods are grown. ZnO arrays can be grown using epitaxy, either heteroepitaxy with appropriately oriented single-crystalline substrate ($MgAl_2O_4$, GaN or Al_2O_3) or homoepitaxy with ZnO thin film deposited on the top of a nonepitaxial substrate (polymer or glass) to act as nucleation layer. In general, seed ZnO layers are required to trigger crystallization of ZnO films on both amorphous or polycrystalline, as well as on single crystal substrates.[26–31]

Despite most work in the field having focused on ZnO nanorods and wires, it has been demonstrated that low-temperature HT deposition can produce high quality films, even epitaxial films. This was first demonstrated by Andeen *et al.*[26,27] by producing epitaxial (0001) ZnO films on the (111) $MgAl_2O_4$ substrates at temperatures as low as 90 °C. Because of close structural relation in this crystallographic setting, ZnO adopts an epitaxial relationship with respect to the substrate. If ZnO film is grown unassisted many islands form on the surface of the substrate and these would grow laterally until they coalesce. To reduce the density of threading dislocations in epitaxial ZnO films photolithography was implemented.[27] Patterning defines the spatial distribution of ZnO islands and thus controls the epitaxial lateral overgrowth process resulting in smooth high-quality (0001) ZnO films. Similar technique was implemented on (0001) GaN single crystal,[32,33] which like ZnO also has a wurtzite structure offering much higher coherency for epitaxial growth of ZnO films. While functional single crystalline layers are easily achieved by epitaxial growth on structurally alike single crystal substrates, producing close approximate of continuous single crystal films on amorphous substrates, such as glass, appears virtually impossible, however, partially oriented growth of ZnO crystals in thin films has been pointed out by Tian *et al.*[30]

The ability to produce ZnO layers on various substrates and its known tendency for growth along the c-axis gave us motivation to attempt a synthesis of dense (0001)-oriented ZnO films on glass substrates that could potentially replace the expensive ITO technology. Here we are facing several challenges such as: (i) obtaining mechanically stable continuous ZnO film without the comfort of epitaxial growth, (ii) achieving dense and transparent ZnO film with low intercrystal porosity, and (iii) producing highly organized polycrystalline texture matching that of the epitaxial films. If all these targets are met then ZnO might soon be used as an inexpensive replacement for ITO glass. In the present work we performed an in-depth study of competitive crystal growth in geometrically confined systems, such as thin films, and exploited its effects for the production of highly oriented, transparent and conductive ZnO thin films on glass substrates.

2. Results and Discussion

The formation of ZnO seed layer is a necessary step in the production of highly adhesive crystalline ZnO films on glass.[20,23] Different geometries of the ZnO seed layer, i.e. film thickness, the size of grains, their connectivity, distribution and crystallographic orientation, strongly influence the final density of the film and consequently its optical and electrical properties. The seed layer must be as thin as possible not to reduce the light transmittance and the grains must be as small as possible to produce ample nucleation sites that statistically maximize the number of (0001)-oriented ZnO grains per unit area of the substrate surface. In our study the seed layers were prepared by calcination of spin-coated Zn-acetate solution (**Figure 1**). The properties of the seed layers were controlled by the concentration of Zn-acetate solution, speed and time of spin-coating; and we are able to control the size of seed grains, their distribution and connectivity with temperature and time of calcination. After heating Zn-acetate solution on glass substrate for 0.5 h at 300 °C a continuous 90 nm thick film is formed. Figure 1a shows an SEM image of the deposited seed layer consisting of 20 nm Zn-acetate grains. The thickness of the deposited layer is controlled by the concentration of the initial Zn-acetate solution. For even thicker layers multiple deposition cycles can be used.[19] This step is followed by calcination to produce dense polycrystalline seed layers of ZnO, shown in Figure 1b. XRD spectra measured after different annealing temperatures showed the appearance of ZnO reflections at as low as 350 °C, which is presently the lowest calcination temperature for the production of continuous ZnO seed layers on glass. Calcination at higher temperatures typically resulted in coarse-grained microstructures, whereas calcination at lower temperatures produces smaller ZnO seed grains, which are also more suitable for the formation of high-quality ZnO films. Without calcination, however, deposited Zn-acetate layer dissolves during the HT treatment and as a result ZnO crystals do not grow on glass substrate, but rather precipitate homogeneously from the solution. In addition to the calcination temperature, the thickness of Zn-acetate layer plays an important role in the connectivity of ZnO grains in the seed layer. Zn-acetate films thinner than 90 nm generally resulted in the formation of discontinuous layers and islands without ZnO film on the glass slide, whereas thicker layers reduced the transmittance of the product. Ideally,

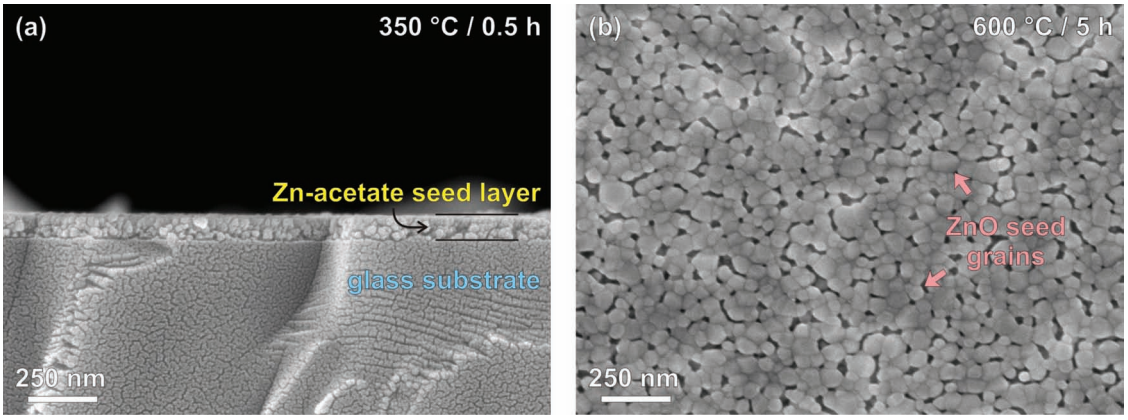

Figure 1. a) Cross-sectional FEG-SEM micrograph of deposited Zn-acetate on glass substrate. b) Seed-layer after calcination at 600 °C for 5 h is composed of highly connected ZnO grains with the size between 40 and 100 nm that serve as nucleation sites for crystal growth during the HT process. The lowest calcination temperature is 350 °C with the average ZnO grain size dropping below 20 nm.

all ZnO crystals in the film should have the same orientation: with their c-axes pointing normal from the substrate to achieve maximal transmittance[33] and grown in a hexagonal close-packed array to minimize the intercrystal porosity.[26,27]

Functional ZnO layers obtained by low-temperature HT treatment of glass substrates with ZnO seed layers are shown in **Figure 2**. When ZnO is grown from Zn-nitrate solution dense arrays of needle-like ZnO crystals are developed (Figures 2a,b). The resulting layers consisted of acicular ZnO crystals reaching the lengths of 17 μm and widths of approx. 300 nm. Near the substrate the crystals are smaller and more randomly oriented, whereas those growing perpendicular to the substrate are the

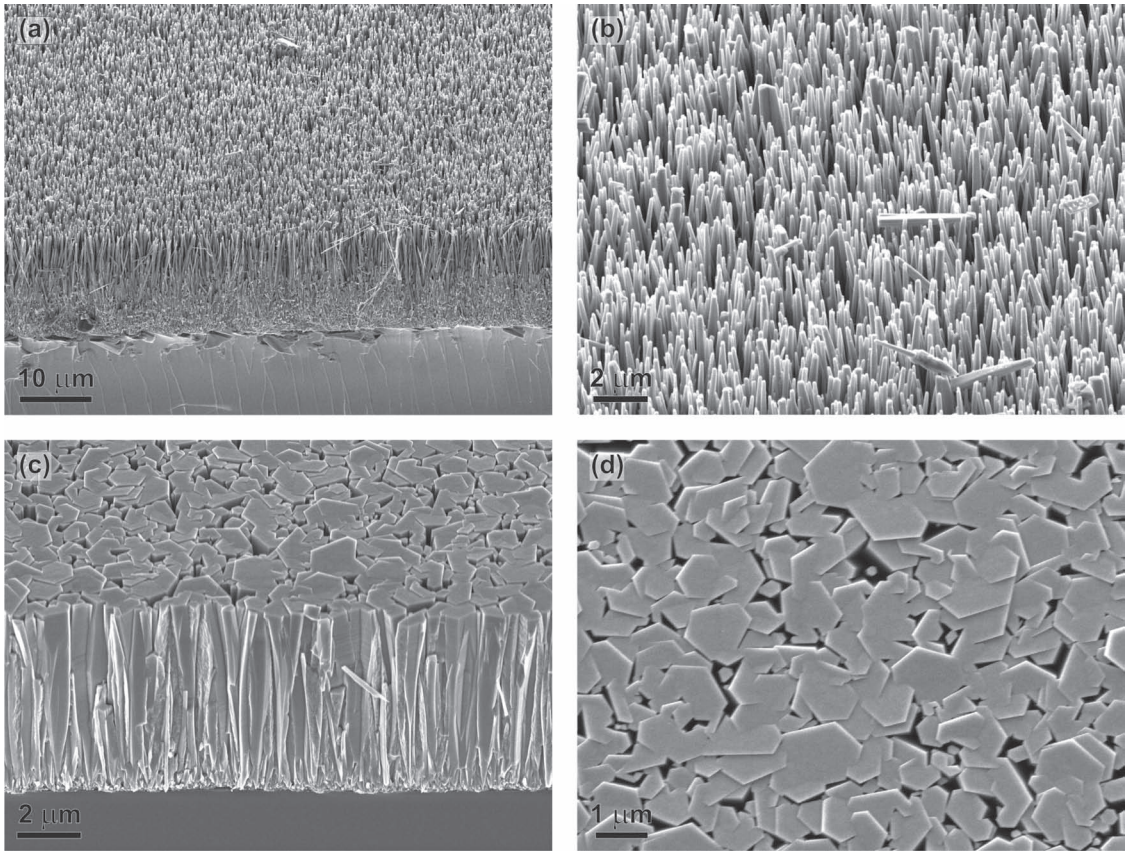

Figure 2. FEG-SEM images of resulting ZnO films after different HT treatments at 90 °C for 18 hours. a) Cross-section and b) top view of ZnO array grown on glass substrate from pure Zn-nitrate aqueous solution. c) Cross-section and d) top view of ZnO film grown from Zn-nitrate solution with the addition of Na-citrate.

longest. Similar textures have been reported for use as piezoelectric nanogenerators,[6] but as such they are not really useful for optical applications, where the layer must emulate optical properties of a single crystal. By using nanocrystalline seed layer we maintain dense nucleation of ZnO crystals, however to produce an optical quality film the morphology of ZnO crystals has to be modified in such a way that the growth rate in [0001]-direction is reduced, or that the growth rate in the prism directions is promoted. For this purpose citrate ions in form of Na-citrate are commonly used.[30] By adding Na-citrate under otherwise identical HT conditions we managed to prepare ZnO layers that were smooth and dense (Figures 2c,d). The films are half thinner compared to the ZnO films prepared without the addition of the citrate ions, whereas the individual ZnO crystals are approx. 3-times thicker. This implies that the citrate ions not only inhibit the growth in [0001]-direction, but even promote the growth of ZnO in prism directions. Similar as in the citrate-free experiment the crystals near the seed layer are small and randomly oriented, and those grown perpendicular are the largest. In cross-section view in Figure 2c it can be seen that after few-hundreds of nanometers the perpendicularly grown crystals already dominate the texture. The surface of the ZnO film, grown by the assistance of citrate solution, shows a close-packed tiling of highly aligned hexagonal ZnO crystals with few isolated intercrystal channels.

Spatial distribution of crystal orientations in ZnO film, shown in Figure 2c,d, was quantitatively assessed by electron backscatter diffraction (EBSD) mapping. EBSD analysis has shown that ZnO crystals preferentially grow with their c-axis perpendicular to the substrate, whereas there is no evident interdependence of the prism orientations, **Figure 3**. 95% of the mapped area (pores excluded) shows c-axes orientations within ±3° deviation from the substrate normal. A high degree of crystal alignment in the ZnO film, however, holds only for {0001} set of planes (Figure 3a), whereas the prisms, *e.g.* {11$\bar{2}$0} (Figure 3b), are arbitrarily rotated with no orientational preference whatsoever. EBSD maps testify that under particular HT conditions self-alignment of the c-axes of ZnO crystals is successfully accomplished, whereas their rotation remains random.

At first glance, highly oriented texture seems rather unusual for HT growth on amorphous substrate, which by itself passes no structural information that could dictate crystal growth in any specific crystallographic direction. To understand the formation of such microstructure under HT growth conditions we investigated what actually happens in the seed layer where ZnO crystals nucleate. A composite transmission electron microscopy (TEM) image in **Figure 4** shows a cross-section of ZnO film with columnar grains. The texture is dominated by large ZnO grains grown from a seed layer perpendicular to the underlying glass substrate. Electron diffraction pattern (EDP) recorded from the seed layer shows that ZnO grains in this region have completely random orientations among themselves as well as with respect to the substrate. If EDPs are measured on columnar ZnO grains we can see that their c-axes are oriented more or less perpendicular to the substrate, whereas the prism directions are uncorrelated. In regions, where the density of columnar ZnO grains is high, their deviation from the substrate normal is smaller, whereas in the areas of higher porosity we observe a larger count of misoriented crystals. These observations imply that due to their unsuitable orientation most of the grains in the seed layer fail to grow all the way to the top of the film, and only few ZnO grains that have their c-axis oriented most perpendicular to the substrate prevail. This indicates that we must have a sufficient (critical) number of ZnO grains in the primary seed layer that one of them would be suitably oriented (perpendicular to the substrate). The ratio between the area occupied by an average perpendicularly grown large ZnO crystal in the film and that of primary ZnO grains in a seed layer shows that ~300 primary grains were available for orientation-selective growth.

As shown by Tian *et al.*,[30] citrate ions markedly slow down the natural fast growth rate of ZnO along the <0001> directions, however the actual mechanism of this growth inhibition is not well understood. The influence of different non-zinc metal sulfates on the morphology of HT synthesized ZnO nanowires was recently explained by face-selective electrostatic crystal growth.[34] From the reported growth rates of ZnO in different crystallographic directions, where $\vec{r}$ [0001] > $\vec{r}$ [prism] directions > $\vec{r}$ [000$\bar{1}$],[35] one could anticipate that ZnO crystals in our films are (0001) terminated. These growth rates, however, were determined under solid-state growth conditions, and can not be directly compared with low-temperature HT growth, where under different crystallization conditions the growth rates could even be reversed. In order to understand the mechanism of why the citrate molecules bind to the ZnO surfaces we determined the absolute orientation of the c-axis using a modified convergent beam electron diffraction (CBED) method[36,37] and showed that ZnO crystals in our films are in fact Zn-terminated, **Figure 5**. According to

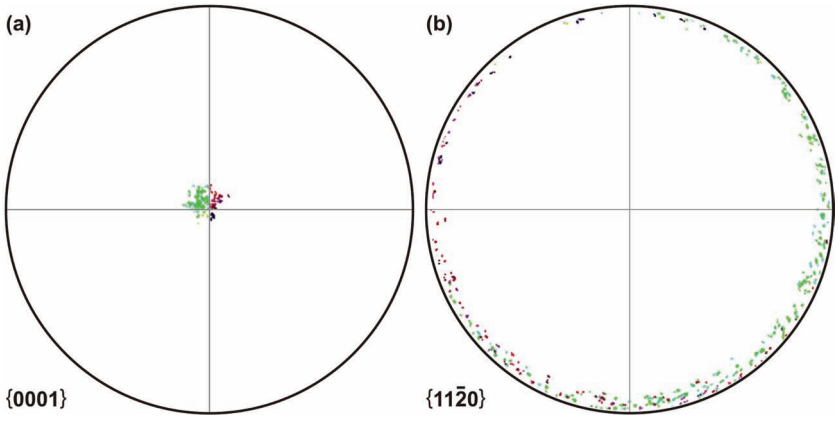

Figure 3. EBSD pole figures showing orientation distribution of ZnO crystals (2040 data points) in layers shown in Figures 2c,d. Central position represents 0° tilt from the substrate normal, whereas the circumference represents 90° tilt of measured pole from the normal in both x and y directions. a) C-axis plot shows that majority of the crystals have their basal {0001}-planes oriented within ±3° with respect to the substrate surface and accordingly b) the majority of prism {11$\bar{2}$0}-planes are oriented perpendicular to the substrate. The small offset from the centre is due to misalignment of the sample in FEG-SEM.

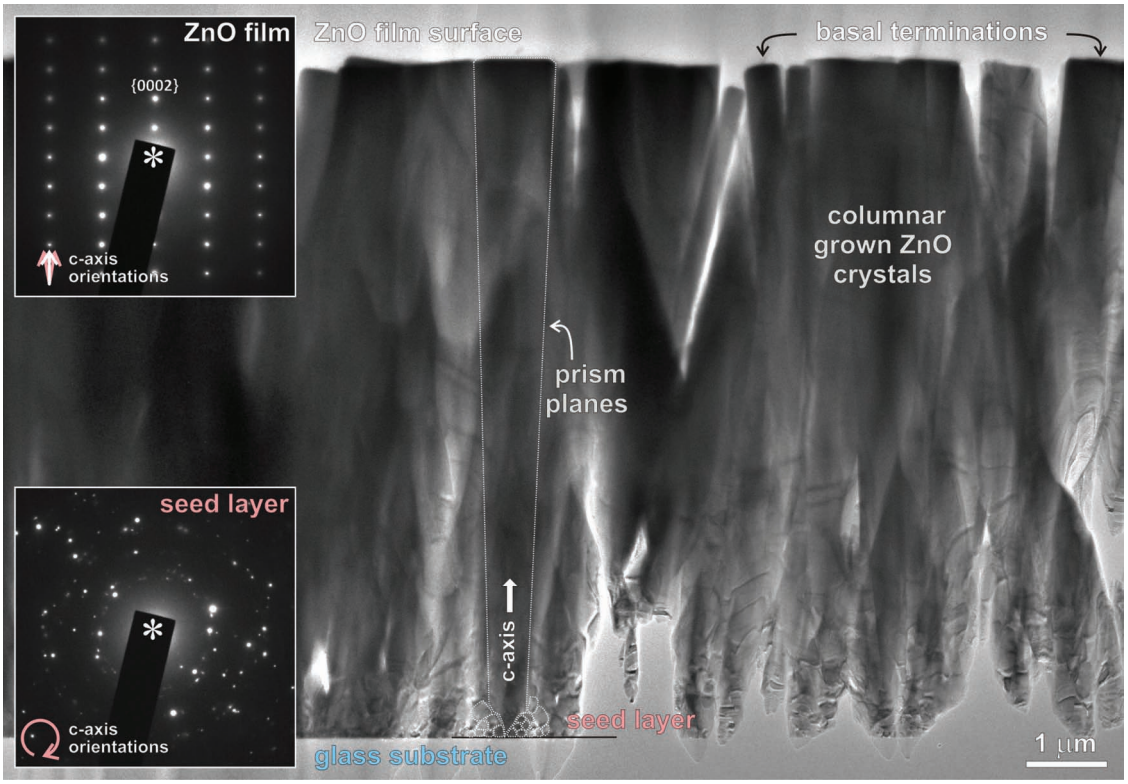

Figure 4. Cross-sectional TEM image of crystalline ZnO film on glass substrate with corresponding EDPs recorded from the seed layer (lower left corner) and from columnar ZnO grain grown all the way to the film surface (upper left corner). The film surface is dominated by flat {0001} terminations of large ZnO crystals grown during HT treatment in the presence of citrate ions.

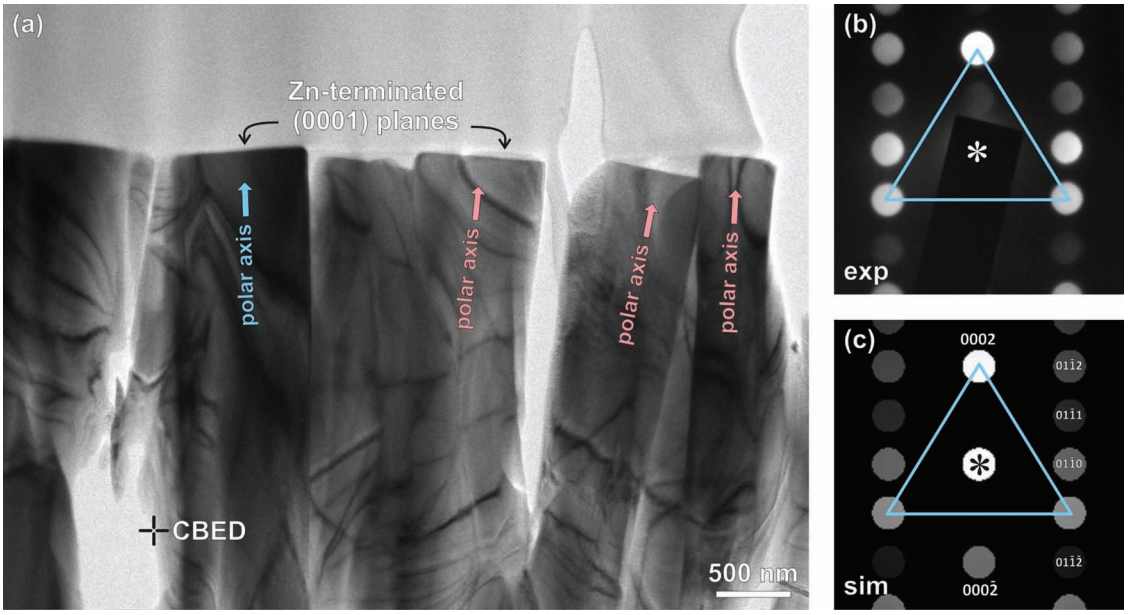

Figure 5. Determination of crystal polarity of HT grown columnar grains in ZnO film on glass substrate in the presence of citrate ions. a) The cross-sectional TEM image of columnar ZnO grains grown on glass substrate and position of the CBED experiment on a crystal tilted in [11$\bar{2}$0] zone axis with resulting b) microdiffraction pattern and c) simulated CBED pattern based on ZOLZ Bloch-wave computation. The experiment shows that under particular synthesis conditions ZnO grains grow in the positive [0001] direction of the c-axis.

the non-centrosymmetric nature of the ZnO structure positive pedion (0001) is Zn-terminated, whereas its negative counterpart (000$\bar{1}$) is O-terminated. Selected ZnO crystal, marked in Figure 5a, was carefully tilted into a zone axis [11$\bar{2}$0], containing polar c-axis related reflections. Differences in the intensities of Bijvoet-related pairs **g** and **–g**, caused by dynamical interactions of zero-order Laue zone (ZOLZ) reflections, reveal non-centrosymmetric character of the ZnO crystal. By moving the incident electron beam from a specimen hole into thin crystal region we can observe gradual changes in beam intensities. The most prominent is the change of the polar reflections where in up to 20 nm thick crystal (0002) beam has a consistently higher intensity than its (000$\bar{2}$) counter pair. By comparison of experimental microdiffraction pattern (Figure 5b) and computed CBED patterns[38] for identical set of electron-optical parameters (Figure 5c) we can confirm that columnar ZnO grains in the film synthesized on glass substrate under HT conditions in the presence of citrate ions grow along the [0001] direction and that the basal planes composing the surface of the ZnO film are Zn-terminated. Exposed Zn-terminating surfaces, where positively charged Zn atoms are distributed in an ordered three-fold pattern, offer convenient adsorption sites for dissociated citrate ions ($[C_3H_5O(COO)_3]^{3-}$). Negatively charged carboxyl groups (COO^-) can freely rotate about the single bonds to adopt the Zn-triplets with interatomic spacing of 0.335 nm. By adsorption on Zn-terminating surfaces large citrate ions hinder in-plane crystallization of ZnO by increasing diffusion paths for growth, whereas prism planes grow freely as they remain unaffected. By adding higher concentrations of the citrate ions to the solution, the growth in [0001] direction is additionally hindered by the electrostatic repulsion of $[Zn(OH)_4]^{2-}$ ions by dangling negatively charged carboxyl groups that are not attached to Zn atoms on the ZnO surface.[27,39]

With all this in mind we can explain this orientation-selective mechanism that leads to the formation of smooth and dense (0001) oriented ZnO film. There are several conditions that must be met for such mechanism to come into play: (i) polycrystalline seed layer, (ii) anisotropic crystal growth and (iii) growth in 2D geometry (thin film). The seed layer serves as a nucleation site for the columnar grown ZnO crystals. According to our observations only ZnO grains with their c-axis oriented perpendicular or nearly perpendicular to the substrate grew all the way to the top of the ZnO film; all differently oriented ZnO crystals stopped their growth at earlier stages. This implies that there is a strong spatial competition during growth – the crystals oriented perpendicular to the substrate have much better chances to grow longer, whereas all otherwise oriented crystals soon suffer impingements into neighboring crystals and their growth is stopped. The growth direction is defined by the orientation of ZnO grains in the seed layer. We need a critical number of seed grains in order to get one suitably oriented. By choosing the initial grain size in the seed layer we also define spatial distribution of perpendicularly oriented crystals. If the seed grains are smaller we get one suitably oriented grain in a smaller area than if the seed grains are larger. This mechanism is only possible when the crystals grow anisotropically. The ratio between the growth rates along individual crystallographic directions is proportional to the corresponding axial ratio measured from the equilibrium shape of the crystals. Under our experimental conditions the growth rate in [0001] direction is 60-times faster than the growth rate along prism directions in the citrate free system, and only 8-times faster in the system with the citrate addition, being still sufficient for orientational-selective growth to come to an effect.

Another condition for orientation-selective growth is that the crystals are restrained in 2D. Such condition is met during crystal growth in thin films or crystallization in narrow cracks (geology). A flat substrate limits the growth of the crystals from all possible directions to a lateral growth within the substrate plane, and upwards. In lateral overgrowth the only limitation are other crystals that are present on the substrate, so if there are no such obstacles in the close vicinity the crystal can freely grow in-plane. However, if such obstacles exist, especially in seed layers with high lateral density of the crystals, then the only free path for growth is upwards, normal to the substrate. Now it depends on the initial crystal orientation to which direction the crystal is predetermined to grow. If its crystallographic orientation dictates in-plane growth, this crystal will soon impinge into neighboring crystals, however, if its fast growing direction is aligned perpendicular to the substrate then it can grow unrestrained all the way up, as long as surrounding conditions allow crystallization. Substrate therefore reduces one degree of freedom by allowing growth in only two dimensions, whereas anisotropic growth of the crystals along specific crystallographic orientation, spatially limited by neighboring grains, reduce another degree of freedom, so that only the growth direction parallel with the substrate normal remains available. Following orientational-selective growth, only suitably oriented crystals survive to the top of the film. The film is finally composed of crystals that all have their c-axes oriented normal to the underlying substrate. Orientation-selective growth due to described spatially confined oriented growth (SCOG) mechanism is illustrated in **Figure 6**. It took place in both processing routes, with and without citrate addition, the only difference is the morphology of the ZnO grains in the two cases. In this way we efficiently control the c-axis orientation, however the remaining task is to control also the rotation of ZnO crystals. One way to reduce the rotational degree of freedom would be introducing self-organization of ZnO seed crystals in the nucleation step, as recently shown by Luković-Golić *et al.*[40] In this way all ZnO grains would be tiled-up into a close-packed 2D hexagonal array prior to HT treatment and growth of ZnO film. As a proof-of-the-concept individual stages of crystal growth according to the SCOG mechanism were experimentally reproduced by HT growth of ZnO crystals on isolated dots of seed ZnO grains, as shown in **Figure 7**.

Films with acicular ZnO crystals (*see* Figures 2a,b) are visually opaque. Consequently, the films untreated with Na-acetate show almost no transmittance. No transmittance results from the increased scattering of photons by the isolated ZnO rods. In dense crystalline films synthesized in the presence of citrate ions (*see* Figures 2c,d) the transparency is rapidly improved mainly due to high coalescence of ZnO crystals through SCOG mechanism. The transmittance spectra are shown in **Figure 8**a. Depending on the preparation of the seed layer the transmittance in the visible range of the spectrum for these films varied from 82% to 72% at 450 nm. These values are reaching the reported values of ITO-coated PES substrates with 82%,[41] or

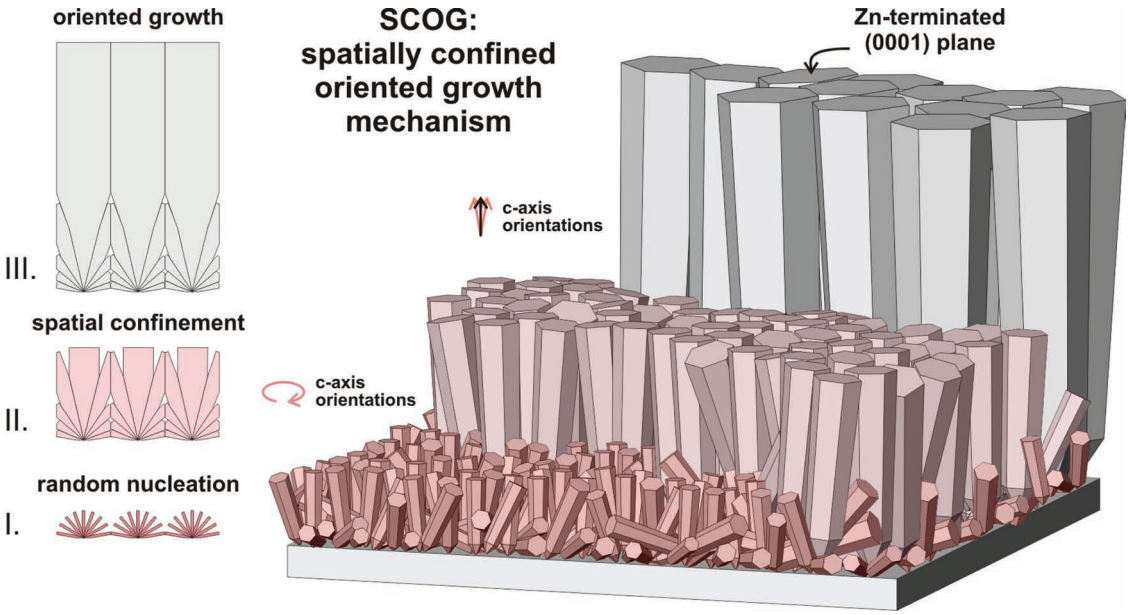

Figure 6. Schematic illustration of ZnO film growth following the spatially confined oriented growth (SCOG) mechanism. Stage I, ZnO crystals have a preferential growth direction along the positive direction of the c-axis and all grains in the early stages of growth start to grow in this direction. Stage II, crystals that are not oriented with c-axis perpendicular or close to perpendicular to the substrate soon impinge to other crystals in surroundings and their growth is stopped. And finally Stage III, only the crystals oriented close to the substrate normal survive. A simplified sketch of the three growth stages is shown on the left side of the illustration.

GaN-buffered Al_2O_3 (0001) substrate with 75%.[32] The difference in the transmittance is due to different initial grain size in the seed layers prior to HT synthesis. Namely, larger initial grains in the seed layer offer fewer suitable orientations for orientational selective growth and ZnO crystals in such layers grow longer in disordered manner (II. stage of the SCOG mechanism) than in the case with higher number of nuclei within the same area of the seed layer. Under conditions of extended II. stage of SCOG the band of disoriented grains in the film is thicker and this consequently produces more boundary associated defects that cause more phonons to scatter and hence the transmittance is lower. 82% transmittance for an 8 µm thick polycrystalline ZnO film grown on glass substrate is in fact a fascinating result compared to the transmittances reported by other authors for only up to 150 nm thick ZnO films, prepared by other deposition methods, with poor conductances and dramatically decreased transmittances with the increasing film thicknesses.[14,19,24]

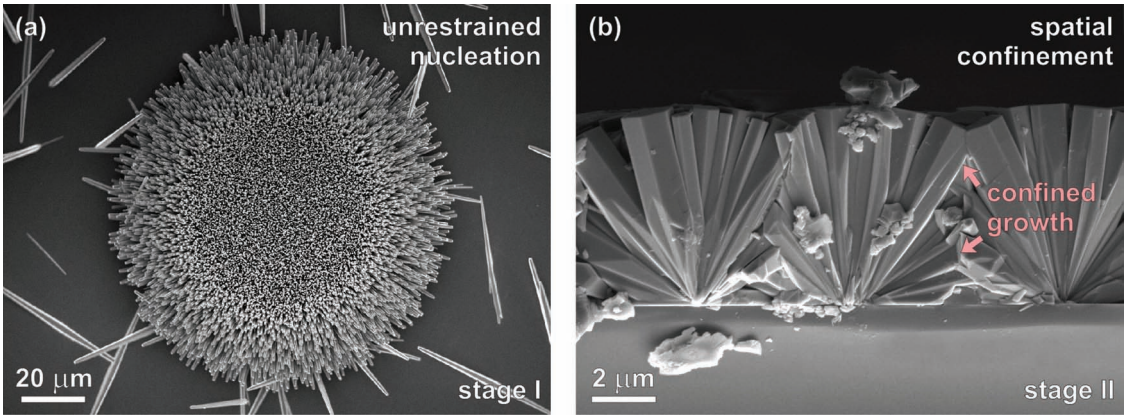

Figure 7. Initial stages of SCOG mechanism. a) Unrestrained nucleation of acicular ZnO crystals on an isolated dot of seed grains ink-jet printed, with an initial diameter of 50 µm. Top view shows that in the centre of the dot ZnO crystals grew perpendicular to the substrate due to spatial confinement for lateral growth, while crystals at the edge of the dot grew laterally as there were no spatial limitations in that direction. b) Spatial confinement becomes important when the mean free path between the nucleation sites becomes smaller than the length of the ZnO crystals. The side view shows three bundles of ZnO crystals grown from nucleation dots separated by 5 µm. As this distance is smaller than the length of the crystals lateral impingement of unsuitably oriented crystals occurs (*see* illustration for SCOG mechanism of orientational-selective growth in Figure 6).

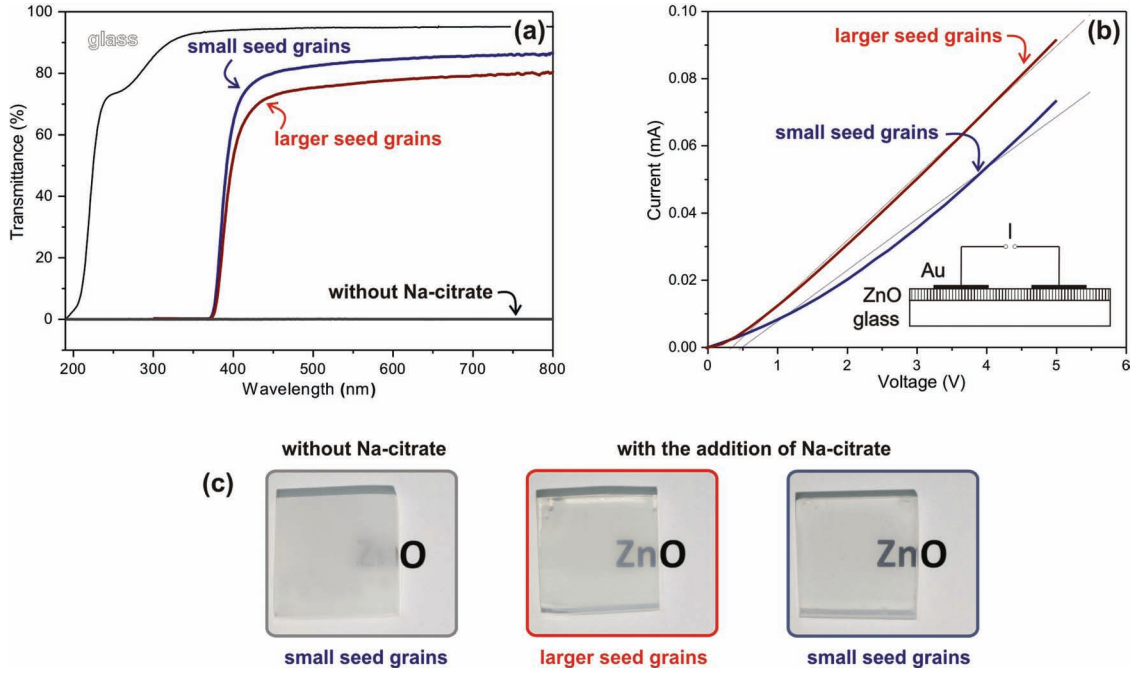

Figure 8. Optical and electrical characterization of ZnO films on glass substrates. a) Room temperature transmittance spectra of empty glass substrate, glass substrate coated with ZnO film after HT synthesis in the presence of citrate ions grown on two different seed layers: the one calcinated at 350 °C for 5 hours (smaller seed grains), and the other annealed at 900 °C for 30 min (larger seed grains) and glass substrate coated with arrays of acicular ZnO crystals grown without the addition of Na-citrate during HT synthesis. b) *I–V* curves with linear fits for transparent ZnO films measured with 2-points measurement; ZnO films were prepared on seed layers with larger and smaller seed grains. The inset shows schematic sketch of the 2-point measuring device. c) ZnO films on glass substrates prepared from smaller or larger seed grains and without or with the addition of Na-citrate. The width of the glass substrates with ZnO films is approx. 15 mm.

In addition to transmittance, ZnO films were measured for their electrical conductivity. ZnO is an intrinsic semiconductor.[2] It exhibits a n-type conductivity attributed to the presence of point defects, such as oxygen vacancies and interstitial Zn atoms. The reliable p-type semiconductor of intrinsically doped ZnO (by varying stochiometry, for example) is still a matter of debate. However the aim of this work was to show how ZnO films can be used as a transparent electrodes and an exact transport mechanism is from this point of view irrelevant. For this reason we only measured *I–V* characteristics to estimate the specific resistivity. A simple two-point measurement gave an estimate for specific resistivity to be of the order of few 10^{-1} Ωcm (*I–V* characteristics are shown in Figure 8b along are the linear fits), which is almost two orders of magnitude lower than the average values for undoped ZnO ceramics. Furthermore, the resistivity of the films does not change over a long period of time. This unusually low resistivity is still not understood. Similarly low resistivities were obtained for intrinsically doped ZnO by manipulating Zn and O stoichiometry, however the exact structural reasons were not given.[42] Four-point measurement of specific resistivity did not result in significantly different values compared to those measured by the two-point method. Because of the unclear electric field geometry our measurements are merely estimations for highest possible values, *i.e.* the actual resistivities of the films can in fact be lower. For this reason usually the sheet resistance is specified and for our film it is in the order of few 100 Ω sq^{-1} regardless of the used method. These values are closer to the values typical for single crystal semiconductors rather than ceramics.[43] With suitable doping (Al) ZnO conductivity could be further improved.[18,44] On the other hand, unintentional intrinsic (Zn and O) or extrinsic (Na) heavy doping could also result in the increase of conductivity.[43,45] But for a film with our values for transparency the resistivity is significantly higher than any so far reported data.[14,19,24] This difference could be explained by highly oriented texture and high coalescence of ZnO single crystals in our films grown via SCOG mechanism, where electron and photon scattering sites, for charge and light transport respectively, have to be heavily quenched.

3. Conclusions

In the present work dense, highly transparent and conductive (0001)-oriented ZnO films on glass substrates were synthesized via low temperature hydrothermal route exploiting basic principles of crystal growth in confined geometries. In order to grow such highly oriented polycrystalline films on amorphous substrates via SCOG mechanism three necessary conditions must be fulfilled: (i) we need a high number of nucleation sites (seed layer) in the first stage of growth, (ii) crystals must exhibit high anisotropy, (iii) growth must be limited to 2D geometry (thin film). This mechanism was demonstrated on fabrication of ZnO films on glass substrates showing high transparency and

conductivity which meet the high standards for many photonic and/or electronic applications.

4. Experimental Section

Synthesis: ZnO arrays and films on glass substrates were synthesized by low-temperature aqueous solution route using Zn-precursor solutions. Seed ZnO layers were manufactured in the following way. Zn-acetate solutions (0.5 M and 0.25 M) were prepared by a dissolution of zinc acetate dehydrate [$Zn(CH_3COO)_2.2H_2O$] (Sigma-Aldrich) in a mixture of absolute ethanol and diethanolamine [$C_4H_{11}NO_2$] (Sigma-Aldrich). The solution was spin coated at 3000 rpm for 30 s (KW-4A, Chemat Technology, California) on a high temperature glass substrate (Corning Vycor glass slide No. 7913), cleaned by rinsing in soap/water mixture, diluted HNO_3 (1:4), acetone and ethanol, and then dried in an oven at 100 °C for 1 hour prior to deposition. As-deposited Zn-acetate layer was heated at 300 °C for 30 minutes to remove the residual solvents and finally calcinated at temperatures between 350 to 900 °C for different times to produce fine grained ZnO layers. For isolated dots of seed ZnO grains we used an ink-jet printing technique of Zn-acetate solution by piezoelectric ink-jet printer (Dimatix DMP2831, Dimatix Fujifilm, Lebanon, NH). After calcination, as-prepared ZnO seed-layers were used for nucleation in the subsequent crystallization process. For the HT synthesis of ZnO films an aqueous solution of Zn-nitrate was used.[27,31] The autoclave (perfluoroalkoxy-Teflon digestion vessel, Savillex, California) was filled with aqueous solution (24 ml) of zinc nitrate hexahydrate (0.2 g) [$Zn(NO_3)_2.6H_2O$] (Fisher Chemicals) with or without sodium citrate dihydrate (0.05 g) [$Na_3C_6H_5O_7$] (Sigma-Aldrich) as a crystal morphology-controlling agent.[30] The pH of the solution was adjusted to 10.8 by ammonium hydroxide [NH_4OH] (Acros) in order to control the solubility that ZnO forms as the solution is heated.[27,30,39] Glass substrates with ZnO seed-layers were mounted into an autoclave facing downwards to avoid precipitation of loose ZnO crystals from the solution. After HT treatment for 18 h at 90 °C, the substrate with grown ZnO film was removed from the solution, rinsed in deionized water and blow-dried by compressed air. The samples were additionally annealed at 250 °C for 1 hour to improve conductivity.

Microstructural Characterization: The surface and the cross-sections of seed layers and deposited ZnO films and arrays were investigated by FEG-SEM (model FEI XL30, Philips, Eindhoven, Netherlands). Micrographs were used to measure various microstructural features such as grain size, film thickness, crystal morphology and pore distribution. The spatial distribution of crystallographic orientations of the ZnO grains grown in the films was studied using a technique (EBSD; Oxford Instruments HKL system with a Nordlys EBSD detector and a Channel 5 software) installed into a FEG-SEM (model JSM-7600F, JEOL Inc., Tokyo, Japan). EBSD analyses were performed at SEM operating conditions set to 20 kV accelerating voltage, 10 nA beam current, working distance of 20 mm and the specimen tilt of 70°. Because ZnO films are sufficiently conductive no charging was observed on the samples and no carbon-coating was necessary to perform SEM/EBSD analyses. The EBSD patterns were acquired at 70 ms dwell time per point and indexed using the unit cell parameters of hexagonal ZnO (ICSD #94002). Orientation maps were acquired within a frame of 10×15 µm and a step of 0.2 µm between the points. The acquired data were subsequently processed to obtain information about crystallographic orientation of ZnO crystals located in EBSD maps. For TEM, cross-sections of ZnO films were mounted face-to-face into 3-mm-diameter sample supports, ground and dimpled (Dimple Grinder, Gatan Inc., Warrendale, Pennsylvania) to approximately 20 µm in the disk center. The TEM samples were produced by ion-milling (RES 010, Bal-Tec AG, Balzers, Liechtenstein) using 6 keV Ar^+ ions at an incidence angle of 10° until perforation. To determine the absolute orientation of polar c-axis of ZnO crystals CBED method was implemented.[36] Diffraction patterns were recorded using a conventional TEM (JEM 2100, Jeol Ltd., Tokyo, Japan) operated at 200 kV. Experimental microdiffraction patterns were matched to the simulated CBED patterns to obtain the absolute orientation of the ZnO crystals.[37] CBED simulations based on the contributing ZOLZ reflections were performed using a Bloch-wave method (EMS software package, EPFL Lausanne).[38]

Optical and Electrical characterization: Optical properties were measured by UV-Vis-NIR absorption spectroscopy (model Shimadzu 3200, Shimadzu Corp, Tokyo, Japan). The electrical characteristics of the transparent ZnO films were determined using 2-point and 4-point current-voltage characteristics at room temperature (Keithley 238 current source and Keithley 2000 voltmeter, Keithley Corp, Cleveland, Ohio) where flat gold electrodes separated by 5 mm were pressed on top of the film. The gold electrodes were produced using a sputter coater (model SCD 050, BalTec, Balzers, Liechtenstein).

Acknowledgements

Matejka Podlogar is deeply grateful to the late Professor F. F. Lange for his guidance and support during her stay at the Materials Department, University of California Santa Barbara (CA) in 2010. She would like to express her deepest gratitude at having had the chance to work with him.

This work was supported in part by the United States National Science Foundation under Grant No.095254. The visit at the UCSB was additionally supported by Slovene Human Resources Development and Scholarship Fund under Grant No. 11012-7/2010-4. The authors thank Gregor Trefalt for ink-jet printing and Daniel Estrada for his help in lab.

Received: January 23, 2012
Published online: April 30, 2012

[1] Ü. Özgür, Y. I. Alivov, C. Liu, A. Teke, M. A. Reshchikov, S. Doğan, V. Avrutin, S.-J. Cho, H. Morkoç, *J. Appl. Phys.* **2005**, *98*, 041301.
[2] D. C. Look, B. Claflin, Y. I. Alivov, S. J. Park, *Phys. Status Solidi A* **2004**, *201*, 2203.
[3] D. B. Thompson, J. J. Richardson, S. P. DenBaars, F. F. Lange, *Appl. Phys. Express 2* **2009**, 042101.
[4] J. X. Wang, X. W. Sun, Y. Yang, H. Huang, Y. C. Lee, O. K. Tan, L. Vayssieres, *Nanotechnology* **2006**, *17*, 4995.
[5] M. Riaz, J. Song, O. Nur, Z. L. Wang, M. Willander, *Adv. Funct. Mater.* **2011**, *21*, 628.
[6] H.-K. Park, K. Y. Lee, J.-S. Seo, J.-A. Jeong, H.-K. Kim, D. Choi, S.-W. Kim, *Adv. Funct. Mater.* **2011**, *21*, 1187.
[7] J. Wang, J. Sha, Q. Yang, X. Ma, H. Zhang, J. Yu, D. Yang, *Mater. Lett.* **2005**, *59*, 2710.
[8] M. Gabás, P. Díaz-Carrasco, F. Agulló-Rueda, P. Herrero, A. R. Landa-Cánovas, J. R. Ramos-Barrado, *Sol. Energy Mater. Sol. Cells* **2011**, *95*, 2327.
[9] S. Masuda, K. Kitamura, Y. Okumura, S. Miyatake, H. Tabata, T. Kawai, *J. Appl. Phys.* **2003**, *93*, 1624.
[10] R. Triboulet, J. Perrière, *Prog. Cryst. Growth Charact. Mater.* **2003**, *47*, 65.
[11] M. Godlewski, E. Guziewicz, G. Łuka, T. Krajewski, M. Łukasiewicz, Ł. Wachnicki, A. Wachnicka, K. Kopalko, A. Sarem, B. Dalati, *Thin Solid Films* **2009**, *518*, 1145.
[12] W. I. Park, G.-C. Yi, J.-W. Kim, S.-M. Park, *Appl. Phys. Lett.* **2003**, *82*, 4358.
[13] X. L. Chen, B. H. Xu, J. M. Xue, Y. Zhao, C. C. Wei, J. Sun, Y. Wang, X. D. Zhang, X. H. Geng, *Thin Solid Films* **2007**, *515*, 3753.
[14] Y. Jiang, N. Bahlawane, *Thin Solid Films* **2010**, *519*, 284.
[15] N. Nouzu, A. Ashida, T. Yoshimura, N. Fujimura, *Thin Solid Films* **2010**, *518*, 2957.

[16] J. Weng, Y. Zhang, G. Han, Y. Zhang, L. Xu, J. Xu, X. Huang, K. Chen, *Thin Solid Films* **2005**, *478*, 25.
[17] T. Hamada, E. Fujii, D. Chu, K. Kato, Y. Masuda, *J. Cryst. Growth* **2011**, *314*, 180.
[18] M. Sahal, B. Hartiti, A. Ridah, M. Mollar, B. Marí, *Microelectron. J.* **2008**, *39*, 1425.
[19] J. Tellier, D. Kuščer, B. Malič, J. Cilenšek, M. Škarabot, J. Kovač, G. Gonçalves, I. Muševič, M. Kosec, *Thin Solid Films* **2010**, *518*, 5134.
[20] L. Vayssieres, *Adv. Mater.* **2003**, *15*, 464.
[21] S. Li, S. Zhou, H. Liu, Y. Hang, C. Xia, J. Xu, S. Gu, R. Zhang, *Mater. Lett.* **2007**, *61*, 30.
[22] S.-H. Yi, S.-K. Choi, J.-M. Jang, J.-A Kim, W.-G. Jung, *J. Colloid Interface Sci.* **2007**, *313*, 705.
[23] L. E. Greene, M. Law, D. H. Tan, M. Montano, J. Goldberger, G. Somorjai, P. Yang, *Nano Lett.* **2005**, *5*, 1231.
[24] G. Kenanakis, D. Vernardou, E. Koudoumas, N. Katsarakis, *J. Cryst. Growth* **2009**, *311*, 4799.
[25] S. Yamabi, H. Imai, *J. Mater. Chem.* **2002**, *12*, 3773.
[26] D. Andeen, L. Loeffler, N. Padture, F. F. Lange, *J. Cryst. Growth* **2003**, *259*, 103.
[27] D. Andeen, J. H. Kim, F. F. Lange, G. K. L. Goh, S. Tripathy, *Adv. Funct. Mater.* **2006**, *16*, 799.
[28] Q. Ahsanulhaq, J.-H. Kim, Y.-B. Hahn, *Nanotechnology* **2007**, *18*, 485307.
[29] J. Y. Park, S.-W. Choi, S. S. Kim, *J. Am. Ceram. Soc.* **2011**, *94*, 978.
[30] Z. R. Tian, J. A. Voigt, J. Liu, B. McKenzie, M. J. McDermott, M. A. Rodriguez, H. Konishi, H. Xu, *Nat. Mater.* **2003**, *2*, 821.
[31] K. Sun, W. Wei, Y. Ding, Y. Jing, Z. L. Wang, D. Wang, *Chem. Commun.* **2011**, *47*, 7776.
[32] J. H. Kim, E.-M. Kim, D. Andeen, D. Thomson, S. P. DenBaars, F. F. Lange, *Adv. Funct. Mater.* **2007**, *17*, 463.
[33] S. P. Fillery, F. F. Lange, *Thin Solid Films* **2010**, *518*, 6022.
[34] J. Joo, B. Y. Chow, M. Prakash, E. S. Boyden, J. M. Jacobson, *Nat. Mater.* **2011**, *10*, 596.
[35] J. S. Lee, S. M. Wiederhorn, *J. Am. Ceram. Soc.* **2004**, *87*, 1319.
[36] W. Mader, A. Rečnik, *Phys. Status Solidi A* **1998**, *166*, 381.
[37] A. Rečnik, N. Daneu, T. Walther, W. Mader, *J. Am. Ceram. Soc.* **2001**, *84*, 2657.
[38] P. A. Stadelmann, *Ultramicroscopy* **1987**, *21*, 131.
[39] J. J. Richardson, F. F. Lange, *Cryst. Growth Des.* **2009**, *9*, 2570.
[40] D. Luković Golić, G. Branković, M. Počuča Nešić, K. Vojisavljević, A. Rečnik, N. Daneu, S. Bernik, M. Šćepanović, D. Poleti, Z. Branković, *Nanotechnology* **2011**, *22*, 395603.
[41] J. H. Kim, D. Andeen, F. F. Lange, *Adv. Mater.* **2006**, *18*, 2453.
[42] G. Xiong, J. Wilkinson, B. Mischuck, S. Tüzemen, K. B. Ucer, R. T. Williams, *Appl. Phys. Lett.* **2002**, *80*, 1195.
[43] K. Ellmer, *J. Phys. D: Appl. Phys.* **2001**, *34*, 3097.
[44] J. Zhang, W. Que, *Sol. Energy Mater. Sol. Cells* **2010**, *94*, 2181.
[45] T. K. Gupta, *J. Mater. Res.* **1992**, *7*, 3280.